

SIMULATION OF VEHICLE SPEED AND APPLIED TEMPERATURE EFFECTS ON STRESS LEVEL OF PAVEMENT STRUCTURE

ATABEK BAZARBAEV^{1,2}, AI CHANGFA^{1,2}, BEKHZAD YUSUPOV^{1,2}, YANJUN QIU^{1,2}

¹*School of Civil Engineering, 2Highway Engineering Key Laboratory of Sichuan Province,*

²*Southwest Jiaotong University, Chengdu 610031, China*

Corresponding author's email: otash7348@gmail.com

***Abstract:** Top-down crack (TDC), as an essential aspect of asphalt pavements fatigue life, is one of the major distresses affecting the long-term performance of asphalt concrete pavement. The surface of asphalt pavements is referred as a place where the TDC initiates and propagate downward in relatively short period depending on how extreme the effecting factor is. In the present work, with the aim to enlighten the effecting factor, different speed of vehicle and weather condition (temperature) effects on a stress intensity factor are investigated. The effects of the temperature on the stress intensity factor in the 2nd mode was considerably higher than that in the 1st mode as we as the effect of the different speed.*

***Keywords:** Top-down crack, stress intensity factor, moving load*

I. INTRODUCTION

Top-down cracking is a primary fatigue cracking and widespread mode of failure in asphalt concrete pavement. Top-down cracking occurring at the surface of asphalt concrete layer and gradually propagating downward, has been considered as one of the major distress modes that have a significant effect on the service life of asphalt pavements. It was highlighted that more than 90% of cracking in asphalt pavements is in the form of top-down cracking (Roque, R., Birgisson, B., Drakos, C., & Dietrich, 2004). Therefore, it is imperative to provide guidance for pavement engineers to select hot-mix asphalt (HMA) mixtures and pavement structures that are most resistant to top-down cracking in specified loading and environmental conditions. Several researches have highlighted (Rahman et al. 2017, Schorsch et al. 2003) that the major causes of top-down cracking on a top layer of HMA could be described by material characteristics, pavement structure and traffic load.

Among the above-described cases, the thermal loading and high tensile strains induced by tires at pavement surface are the most recognized and influencing factor that contributes to this failure mechanism. It has also been reported that the pavement structure has little effect on the reduction of tensile stresses around tire-pavement contact area and that the major influencing factor is the distribution of the contact stresses around the tire. In addition, it is generally agreed that the load-induced surface tension could be investigated by dividing into two components of the stress such as longitudinal and transversal. There are few generally accepted approaches to

understand the causes of TDC, however, determining the effecting factors that engage its potential is essential to specify those causes and to find out up to what extent each cause could be valid. Therefore, conducting a study on the availability and validity of different types of crack causes is essential. Finite element method (FEM) can be given as one of those availability to validate the crack causes. FEM is a very powerful numerical method based on computer technology to solve differential equations in engineering problems (Strouboulis et al., 2000). FEM has been used to predict dynamic and fracture responses of the pavement structure and to determine the effects of different crack location and loading distances from the middle of the specimen (Souiyah et al., 2009).

With the aim to evaluate the effecting factors on the resulted stress of the asphalt pavement, in terms of the stress intensity factor, this paper focuses on carrying on broad analyses of the effects of external factors like different speed of the moving load and variety of temperatures in an increasing pattern on the stress intensity factor.

II. MATERIALS AND METHODS

Finite element modeling of 3D pavement

There are several types of FEM software such as ABAQUS, ANSYS, LS-DYNA and ADINA to simulate the vehicle-pavement interaction process. In our study, ABAQUS (Liao, 2008) was utilized to demonstrate the simulation model and its process. The following sections will describe in detail how to build three-dimensional (3D) finite element model of pavement and its basis in commercial software ABAQUS.

The 3D FEM model was developed in ABAQUS and employed to predict crack mechanics of the pavement structure in the present study. The developed 3D FEM could more accurately predict compared to 2D or an axisymmetric model since it contained more features of the pavement, in terms of material properties. However, it would require time consuming and high computational process to carry out. It was assumed that the Z (traffic/movement) direction is along the pavement longitudinal direction, the X direction is perpendicular to the pavement, and Y is in the vertical direction. The length, width and depth of the 3D FEM model were taken with the dimensions of 8m x 6m x 6.5m, respectively. Boundary conditions have essentially significant role in predicting responses of the pavement structure. Therefore, a fixed boundary condition was used at the bottom surface of model. In the other words, all degrees of freedom were restrained with the conditions of $U1=U2=U3=UR1=UR2=UR3=0$. This was $XSMM$ ($U1=UR2=UR3=0$) on left and right sides, and $ZSYMM$ ($U3=UR1=UR2=0$) for the front and rear sides. Tie constraints were used between two adjacent layers. This kind of constraints could provide two surfaces together for the duration of the simulation

Due to the importance of model meshing step in obtaining the most accurate results, many trials were carried out during our simulation to define the best mesh size. In this research, a fine mesh was used to attach the loading area and subsequently, coarse mesh was applied away from the loading area. The main reason for using the coarse mesh away from loading area was to reduce

the total number of elements for achieving time saving. The fine mesh was also implemented around the crack tip area because of large stress occurrence that might happen around the crack tip. This approach results in more accuracy in the analyses of investigation around the crack tip. The defined mesh step was used with an integration unit of C3D8R as shown in figure 2. This type of element could provide better efficiency for simulation performance and high tolerance of distortion for further analysis. The simulation of the developed model with the applied loads in the specific loading area deployed that higher accuracy with smaller computational cost could be obtained by setting correct mesh size and step while carrying out the meshing process. It is mandatory to ensure convergence and assurance of FE model, therefore, a sensitivity analysis, in terms of three different mesh density have been carried out. The resulted sensitivity demonstrated that the total number of nodes were 60276 and there were totally 50668 finite elements model were chosen for meshing and simulation process.

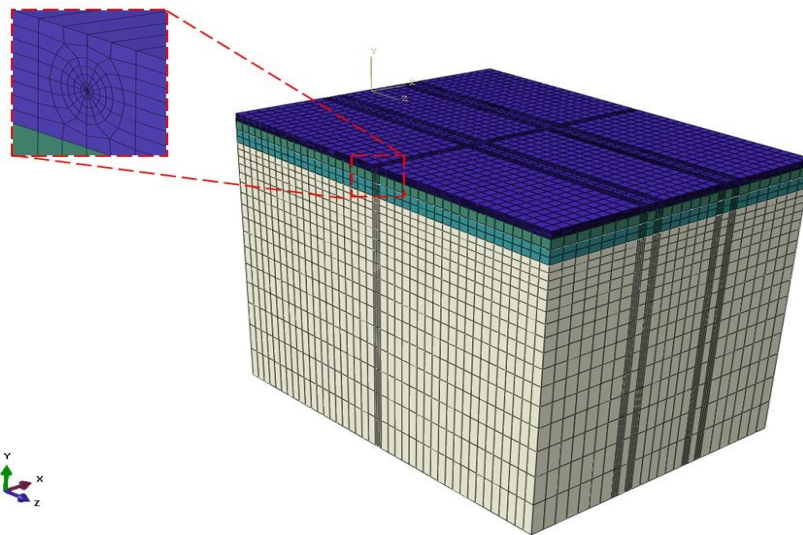


Figure 1. Three-dimensional finite element model after meshing the developed model

Characterization of Moving load Definition

It is necessary that the vehicle load should be accurately applied in the modelling in order to predict crack mechanics of pavement structures (Dinegdae and Birgisson, 2016). Therefore, the dynamic moving load is one of the dominant parameters that should be accurately defined here. A single axle load with double tires was considered to represent the vehicle in the developed model. Realistically, the interaction between the tire and pavement have circular shape. However, in our simulation study, a simple rectangular shape was adopted as a substitution of circle shape due the advantages of the rectangular shape in 3D FEM modelling such as solid elements in mesh generation. On the other hand, using a circular area in full 3D modelling would cause some mesh generation difficulties, especially when solid elements were employed. Figure 3 shows the relationship between rectangular and circular shapes according to a research done by Yang et al. (2017). This method is based on subroutine DLOAD and involves two tools co-simulation of Abaqus/CEA and Fortran language. It should be noted that 0.7 MPa non-uniform pressure was employed in the simulation model.

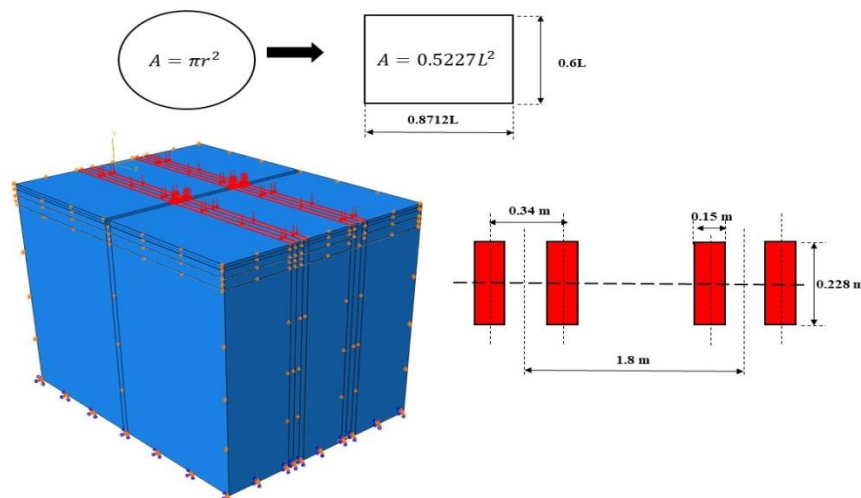


Figure 2. The configuration of moving load in the developed simulation model

Linear elastic behavior of asphalt material

Traditionally, pavement fracture analysis is assumed with elastic solutions that means each pavement material could be considered as elastic material. Besides that, the asphalt material could be characterized with temperature, stress and time dependent material. Several constitutive models have been vastly used in pavement engineering to characterize mechanical behavior of asphalt materials (Miao et al., 2010) with the properties of elasticity, viscoelasticity and viscoelastic plasticity.

In our study, an elastic material behavior was considered to describe of the asphalt material. The elastic material behavior was modelled based on Hooke's. Hooke's law was applied where the stresses were linearly related to the strains. Therefore, each layer was assumed homogeneous, isotropic, and linear elastic. The FEM for describing the behavior of position ratio, young's modulus and density showed a good agreement in Abaqus. The mechanical parameters for different applied temperature cases shown in table 1 were identified based literature sources and model-based analysis.

Table 1. Elastic material properties of the asphalt layer

Name of parameters	5 °C (MPa)	25 °C (MPa)	40 °C (MPa)
E	8930	4750	1790
v	0.23	0.3	0.35

Modeling of material damping

It is essential to use realistic material damping in the nonlinear dynamics modelling (Eshkabilov et al., 2009). The elastic material possesses an energy dissipation source that could be modelled with damping ratio. The damping ration could be defined based on Rayleigh damping matrix [C] as follows:

$$[C] = \alpha[M] + \beta[K] \quad (1)$$

$$\beta = \frac{2\xi}{\omega_1 + \omega_2} \quad (2)$$

where $[M]$ is mass matrix of the model, $[K]$ is stiffness matrix of the model, α is mass proportional damping coefficient and β is stiffness proportional damping coefficient that can be determined from specific parameters such as ξ_i and ξ_j , here the i^{th} and j^{th} modes, respectively. If both modes were assumed to have the same damping ratio ξ , then, those coefficients could be expressed with the following equations:

$$\alpha = \frac{2\xi\omega_1\omega_2}{\omega_1 + \omega_2} \quad (3)$$

$$\beta = \frac{2\xi}{\omega_1 + \omega_2} \quad (4)$$

where ξ is the critical-damping ratio, ω_1 and ω_2 are the natural frequencies defined from modal analysis. Those two frequencies for calculating the Raleigh coefficients may be taken as the first natural frequency of the structure. In addition, for determining natural frequency of model, the first 10th mode shapes to avoid over damping the system were suggested in our case of study.

III. RESULTS AND DISCUSSIONS

As the resulted stress significantly contributes to the occurrence of the crack on the pavement, the causes of the stress can be analyzed based on the effecting factors such as speed of the vehicle and external temperatures (weather conditions). Since the stress on the pavement could be estimated with the stress intensity factor, the relationship between the effecting factors like the speed and weather condition, and the intensity factor could be taken into account to describe the causes. The relationship between the speed of 10 m s^{-1} and intensity factor K_1 , K_2 for the mode 1 and 2 is presented in Fig. 3a and b, respectively. For the speed of 20 and 30 m s^{-1} , the same pattern with slight time shifts and different amplitudes of the intensity factor was observed. Subsequently, the effect of the weather condition, in terms of temperature changes, on the intensity factor K_1 and K_2 at the temperature of 5, 25 and 40°C can be seen in fig. 4 a and b.

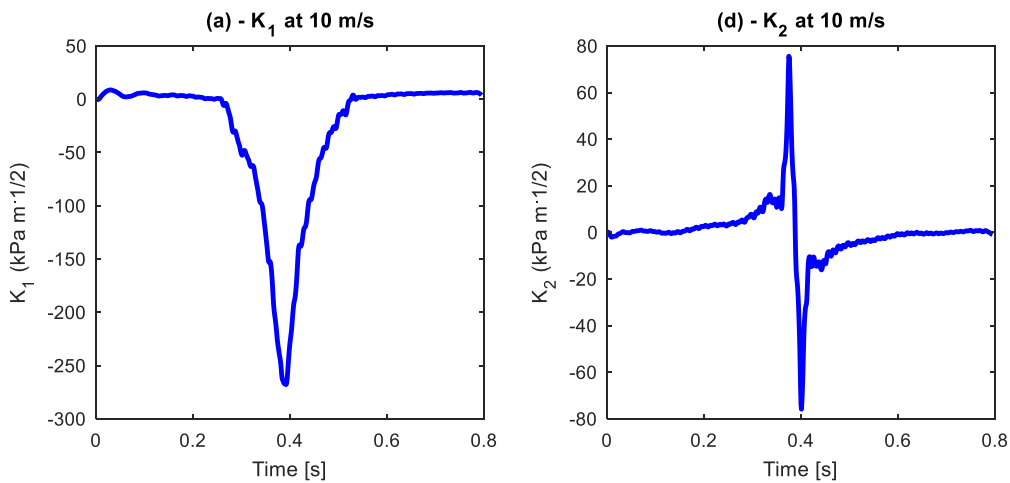


Figure 3. Speed effect on the stress intensity factors K_1 (a) and K_2 (b) at the speed of 10 m/s

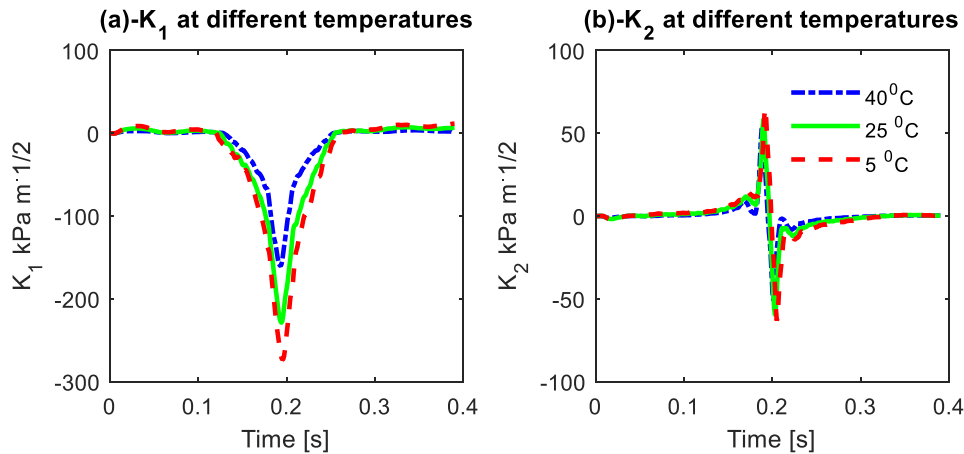


Figure 4. Temperature effect on the stress intensity factors K_1 (a) and K_2 (b) at the temperature of 5, 25 and 40°C

Considering all the effect changes resulted from all applied speeds and temperatures, the effects of the speed and temperatures on the intensity factor can be specified to detect the major changes (fig. 5a and b). The stress intensity factor for the both two modes slightly decreased while the speed of the moving load increased (fig. 5a). In addition, the decrease in the 1st mode was less than that in the 2nd mode. From fig. 4a, it can be noticed that the stress intensity factor for the first mode can be significantly more effected by the temperature change than that for the second mode. This resulted in a considerably higher decrease in the stress intensity factor of the 1st mode than that of the 2nd mode as the temperature increased from 5 to 40°C. Considering all the above-given analyses, it can be stated that the effect of the moving load speed could be higher in the 1st mode. This pattern is opposite for the temperature effect. The stress on the asphalt pavement could be more effected in the 2nd mode.

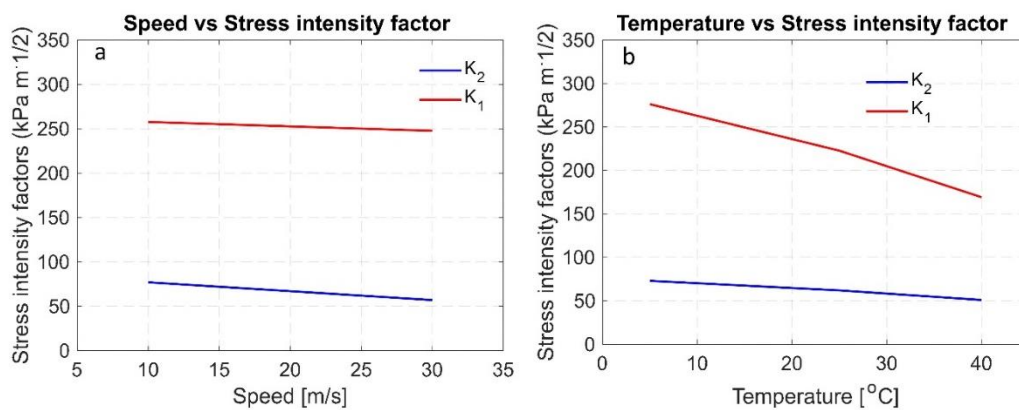


Figure 5. The stress intensity factors vs vehicle speed (a) and temperature (b)

IV. CONCLUSION

A three-dimensional model of the pavement together with its base was developed and the finite element modelling was carried out. The moving load on the developed pavement model was characterized to investigate the effect of different external factors like speed and temperature.

The analyses of the speed and temperature effect on the stress intensity factor revealed that the resulted stress of the pavement, which is the main cause of the crack initiation, was considerably effected by both speed and temperature. The most considerable point to conclude was that the stress was highly influenced by the applied temperatures in the second mode. This finding could be a valuable for further step of the research where increased temperature levels will be tested with the other modes.

References

- [1]. Dinegdae, Y.H., Birgisson, B., 2016. Reliability-based calibration for a mechanics-based fatigue cracking design procedure. *Road Mater. Pavement Des.* 17, 529–546. doi:10.1080/14680629.2015.1094397
- [2]. Eshkabilov, S.L., Kutlimuratov, K., Sharipov, G., Jumaniyazov, H., 2009. Simulation and analysis of cracked beams using finite element analysis and experimental modal analysis methods. *15th Int. Conf. Exp. Mech.* 1–8.
- [3]. Liao, G., 2008. *Application of ABAQUS Software in Road Engineering*. Beijing.
- [4]. Miao, Y., He, T.G., Yang, Q., Zheng, J.J., 2010. Multi-domain hybrid boundary node method for evaluating top-down crack in Asphalt pavements. *Eng. Anal. Bound. Elem.* 34, 755–760. doi:10.1016/j.enganabound.2010.04.002
- [5]. Rahman, M.S., Podolsky, J.H., Williams, R.C., Scholz, T., 2017. A study of top-down cracking in the state of Oregon. *Road Mater. Pavement Des.* 0, 1–25. doi:10.1080/14680629.2017.1345782
- [6]. Roque, R., Birgisson, B., Drakos, C., & Dietrich, B., 2004. Development and field evaluation of energybased criteria for Top-down cracking performance of hot mix asphalt. *J. Assoc. Asph. Paving Technol.* 73, 229–260.
- [7]. Schorsch, M., Chang, C., Baladi, G., 2003. Effects of Segregation on the Initiation and Propagation of Top-Down Cracks 82 nd Transportation Research Board Annual Meeting. *Transp. Res.* 7361.
- [8]. Souiyah, M., Muchtar, A., Alshoaibi, A., Ariffin, A.K., 2009. Finite element analysis of the crack propagation for solid materials. *Am. J. Appl. Sci.* 6, 1396–1402. doi:10.3844/ajassp.2009.1396.1402
- [9]. Strouboulis, T., Babuška, I., Copps, K., 2000. The design and analysis of the Generalized Finite Element Method. *Comput. Methods Appl. Mech. Eng.* 181, 43–69. doi:10.1016/S0045-7825(99)00072-9
- [10]. Yang, L., Wang, P., Wu, T.W., 2017. Boundary element analysis of bar silencers using the scattering matrix with two-dimensional finite element modes. *Eng. Anal. Bound. Elem.* 74, 100–106. doi:10.1016/j.enganabound.2016.11.001